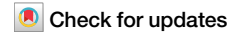




Trophic niche partitioning in giant clams



Isis Guibert ¹, Inga Elizabeth Conti-Jerpe ², Leonard Pons ^{1,3}, Kuselah Tayaban ⁴, Sherry Lyn Sayco ^{4,5}, Patrick Cabaitan ⁴, Cecilia Conaco ⁴ & David Michael Baker ¹

Ecosystems are influenced by competition for limited resources, a driver of niche partitioning. Over time, the emergence of novel traits facilitating new resource exploitation can reduce competition. However, additional layers of complexity, like symbiosis, complicate our understanding of the patterns shaping reef communities. Therefore, empirical evidence of niche partitioning reducing competition in symbiotic benthic communities is limited. Using a unique common garden experiment, we examined the nutritional strategies of six giant clam holobionts and characterized their symbiont assemblages. Variation in trophic strategies confirmed trophic niche partitioning, as species fell along a continuum from highly heterotrophic to highly autotrophic. *Tridacna gigas* and *T. derasa*, listed as critically endangered and endangered, respectively, were the most autotrophic and fast-growing species. We found significant phylogenetic signals in trophic niche scores, growth rate, and shell length, indicating the role of natural selection in shaping giant clam nutritional ecology. We conclude that niche partitioning is a driver of giant clam evolution with benefits and costs; high autotrophy reliance results in greater growth rates yet may increase vulnerability to disturbances. Given the impact of human activities on giant clams, conservation efforts should focus on these ecosystem engineers, especially highly autotrophic and geographically constrained species.

Symbiotic relationships between organisms from different kingdoms serve as a source of evolutionary innovation leading to adaptive strategies. The concept of niche partitioning postulates that competition between species for scarce resources applies evolutionary pressure, resulting in new nutrient-acquisition adaptations¹. Microbial partners can participate in the host's survival, reproduction, protection, and/or resource access^{2,3}. For example, symbiotic interactions between autotrophic (e.g., photo- or chemosynthetic such as green algae or nitrogen-fixing bacteria) and heterotrophic (e.g., host consumers) organisms enable them to overcome nutritional constraints by increasing their resource access⁴. Symbiosis, therefore, provides opportunities for resource partitioning by varying the reliance on autotrophy and heterotrophy, ultimately promoting species coexistence within an ecosystem⁵.

Coral reefs are home to unparalleled biodiversity, much of which is dependent on associated microbiomes to meet energetic requirements for growth and reproduction in a nutrient-poor environment⁶. Symbioses thrive in these oligotrophic benthic habitats, as nutritional symbioses, or trophic symbioses, confer a competitive edge over non-symbiotic species (e.g., obligate suspension-feeding invertebrates). Many marine invertebrate holobionts (i.e., a host and associated microbial symbionts) found on reefs, such as corals and giant clams, are associated with dinoflagellate algae from

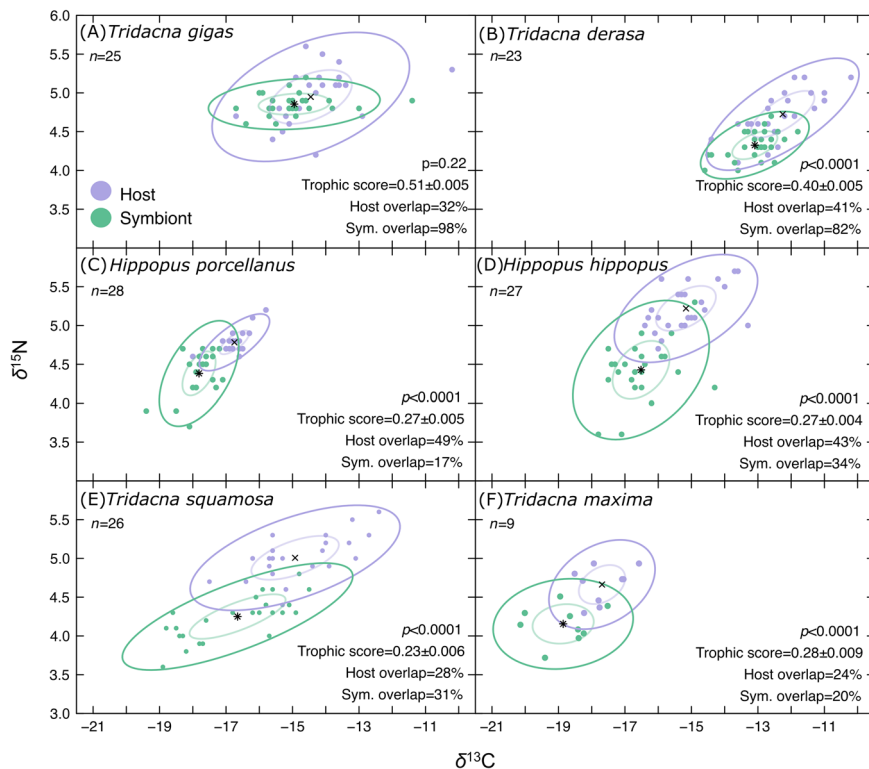
the Symbiodiniaceae family. This association allows the heterotrophic host to access inorganic carbon (e.g. carbon dioxide) and nitrogen (e.g. nitrate) in exchange for metabolic wastes, leading to a recycling of these nutrients within holobionts^{7,8}.

Symbiosis can introduce additional variation into the trophic niches of holobionts through association with different symbionts⁶. Indeed, genera and species of Symbiodiniaceae fit into different ecological niches, including those structured by temperature⁹ and nutrient availability¹⁰. As a result, hosting different symbiont species can confer considerable advantages to the host. Recent evidence suggests that across holobiont taxa, dependence on symbiont-derived nutrition varies along a spectrum that ranges from a high dependence on autotrophy to predominant heterotrophy¹¹. Niche partitioning along this continuum contributes to the coexistence of similar species on reefs. However, this has only been explored in a few taxonomic groups, and evidence for evolutionary niche partitioning within these taxa is limited¹².

This scarcity of research extends to giant clams (subfamily Tridacninae), which represent understudied holobionts despite their conspicuous presence and crucial ecological role. These iconic symbiotic coral reef invertebrates act as ecosystem engineers, providing food sources, substrate, and shelter for a diversity of reef organisms^{13,14}. Consisting of only 12 species

¹Swire Institute of Marine Science, The University of Hong Kong, Hong Kong SAR, China. ²Science Unit, Lingnan University, Hong Kong SAR, China. ³Tropical & Subtropical Research Center, Jeju Research Institute, Korea Institute of Ocean Science & Technology, Jeju-si, Jeju-do, Korea. ⁴Marine Science Institute, University of the Philippines, 1101 Quezon City, Philippines. ⁵Department of Biology and Environmental Science, College of Science, University of the Philippines Cebu, Gorordo Avenue, 6000 Cebu City, Philippines. e-mail: dmaker@hku.hk

Fig. 1 | SIBER analysis of paired giant clam host and associated algal symbiont stable isotope values. Host are represented in purple and associated algal symbiont in green. In total, 6 species are represented: A *Tridacna gigas*, B *Tridacna derasa*, C *Hippopus porcellanus*, D *Hippopus hippopus*, E *Tridacna squamosa* and F *Tridacna maxima*. Lines represent ellipse areas corrected for sample size set to encompass 40% (standard ellipse area; SEA) and 95% (major ellipse area; MEA) of the variation of each group. Black symbols represent the centroids of host (*) and symbiont (x) ellipses. *P*-values < 0.05 generated from residual permutation procedures indicate species where host and symbiont occupy distinct isotopic space. The *n* number of biologically independent samples is indicated by *n* = under each species name. Mean trophic niche score \pm 89% credible intervals indicate where species fall along the heterotrophy (0) - autotrophy (1) gradient. The percentage of overlap of host and symbiont MEAs was calculated using the mode of the last 100 posterior ellipses areas generated in a Bayesian analysis.



across two genera, the phylogenetic relationships of Tridacninae are comprehensively mapped^{15,16}. Their biogeography varies considerably, with a few species occurring broadly across the Indo-Pacific and others restricted to the center of the coral triangle¹⁷. Depending on their location, giant clams can host one or more different genera of Symbiodiniaceae: *Symbiodinium*, *Cladocopium*, *Breviolum*, *Durusdinium* and/or *Gerakladium*^{18–21}. Relatively little is known about the trophic niche of giant clams. The trophic capacity of seven species has been evaluated by prior studies, though no more than four species have been assessed simultaneously, from the same location, nor using the same methods^{22,23}.

In this study, we investigated trophic niche partitioning across six co-occurring species of giant clams, all of similar age and size within each species, sourced from a common garden located in the Philippines. Using Stable Isotope Bayesian Ellipse in R (SIBER) analysis, we quantified nutrient sharing and recycling within giant clams by measuring the overlap between host and symbiont “isotopic niches”, proxies for trophic niche. Giant clam trophic strategies were compared using a recently developed trophic niche index, Host Evaluation: Reliance on Symbionts (HERS), which quantifies the host dependence on associated symbiont nutrition^{24,25}. To gain a holistic picture of trophic niche partitioning in the giant clams, we characterized associated Symbiodiniaceae assemblages with next-generation sequencing. We further assessed whether nutrient sharing and other aspects of clam biology and ecology, such as growth rates and maximum depth, were linked to the phylogenetic relationships between clam hosts. We hypothesized that sympatric clams would exhibit trophic resource partitioning through associations with distinct symbiont assemblages, and that functional traits—including trophic strategy—would produce significant phylogenetic signals, supporting trophic niche partitioning as an evolutionary mechanism that drove divergence and speciation in Tridacninae.

Results

Stable isotope analysis

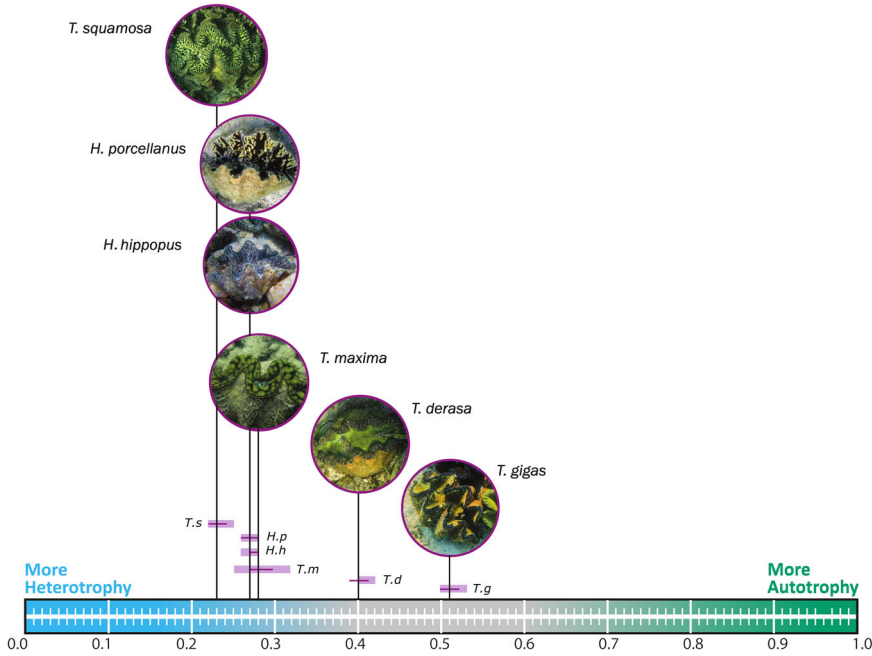
We measured carbon and nitrogen stable isotope values of clam host tissue and associated Symbiodiniaceae in six co-occurring species that were cultured in a hatchery prior to be transplanted in a common garden located in

the Tabunon lagoon (Semirara, Philippines): *Hippopus hippopus*, *Hippopus porcellanus*, *Tridacna derasa*, *Tridacna gigas*, *Tridacna maxima*, and *Tridacna squamosa*. Host stable isotope values were generally higher than those of symbionts; mean $\delta^{13}\text{C}$ ranged between -17.7 ± 0.7 (*T. maxima*) and $-12.3 \pm 0.9\text{‰}$ (*T. derasa*) for clams and -18.9 ± 0.9 (*T. maxima*) and $-13.1 \pm 0.7\text{‰}$ (*T. derasa*) for Symbiodiniaceae while mean $\delta^{15}\text{N}$ ranged between 4.7 ± 0.2 (*T. maxima*) and $5.2 \pm 0.3\text{‰}$ (*H. hippopus*) for clams and 4.2 ± 0.2 (*T. maxima*) and $4.9 \pm 0.1\text{‰}$ (*T. gigas*) for symbionts (Supplementary Table 1). Particulate organic matter (POM) values averaged -18.9 ± 1.7 for $\delta^{13}\text{C}$ and 2.1 ± 1.1 for $\delta^{15}\text{N}$ (Supplementary Data 1).

Overall patterns of nutrient exchange were quantified for each species; however, it is important to note that the sample size of *T. maxima* (*n* = 9) was lower than that of the other species (*n* = 23 to *n* = 28) because fewer individuals were available in the hatchery. While smaller sample size can reduce the precision of the ellipse area estimates, bootstrapped resampling approaches mitigate this pitfall and improve estimate reliability²⁶. We thus present the most robust analysis possible within these sampling constraints, yet we still encourage caution when interpreting the results of *T. maxima* due to its lower sample size.

Differences between host and symbiont isotopic niches across species were explored using SIBER, fitting ellipse areas (EA) to $\delta^{13}\text{C}$ and $\delta^{15}\text{N}$ values on an isotopic biplot (Fig. 1). Only one clam species, *T. gigas*, exhibited overlap (0.29‰^2) between host and symbiont Bayesian Standard Ellipse areas (SEA_B), amounting to 24% of the host (SEA_{BH}) and 90% of the symbiont (SEA_{BS}) SEA_B (Supplementary Table 2). All clam species, however, had overlap between host and symbiont MEAs, ranging from 0.41 (*H. porcellanus*) to 2.31‰^2 (*T. gigas*; Supplementary Table 3). The overlap percentage of host MEA_B (MEA_{BH}) ranged from 24% (*T. maxima*) to 49% (*H. porcellanus*) and exhibited less variation than that of the symbionts (MEA_{BS}), which ranged from 17% (*H. porcellanus*) to 98% (*T. gigas*). The distance between host and symbiont ellipse centroids^{11,27} varied from 0.50‰ (*T. gigas*) to 1.89‰ (*T. squamosa*) across species (Fig. 1). Residual permutation procedures²⁷ demonstrated that host and symbiont groups occupied significantly different space on the isotope biplot for all species (*P* = 0.001; Fig. 1B-F) except *T. gigas* (*P* = 0.116; Fig. 1A).

Fig. 2 | Giant clams trophic niche scores along the trophic strategy spectrum. Scores approaching 0 indicate limited nutrient sharing or recycling between host and symbionts, suggesting the host is more heterotrophic (blue), while score approaching 1 suggest high autotrophy (green). Mean trophic niche scores are indicated by black lines connecting the species to the scale. Lower and upper quartiles of score are indicated by horizontal boxes, and the error bars indicate 89% credible intervals. Individual data points (raw trophic niche scores) for each species are shown in Fig. 3. Pictures: Isis Guibert, drawings: Leonard Pons.



As a final metric quantifying nutrient sharing, we used a trophic niche index (HERS) that incorporated overlap values from both host and symbiont SEA_B and MEA_B to characterize the clams' trophic strategy²⁴. *T. gigas* had a significantly higher trophic niche score (mean=0.51, 89% CI: 0.50–0.52) than all other clams and stood out as the only species with a mean score greater than 0.50 (Fig. 2). The species with the second highest trophic niche score, *T. derasa* (mean=0.40, 89% CI: 0.39–0.41), was significantly higher than all other clams, except for *T. gigas*. *T. maxima* (mean=0.28, 89% CI: 0.27–0.30), *H. hippopus* (mean=0.27, 89% CI: 0.27–0.28), and *H. porcellanus* (mean=0.27, 89% CI: 0.26–0.28) had similar average and scores ranges. *T. squamosa* had a significantly lower trophic score (mean=0.23, 89% CI: 0.22–0.24) than all other clams. Mean growth rates of clam species extracted from the literature¹⁶ were significantly correlated with trophic scores ($R^2 = 0.58$, $P = 0.0471$; Fig. 3). The average growth rate increased with the increase of the trophic niche score for all species, except for *T. maxima*, which displayed the lowest growth rate (1.71 mm/month) despite having an average trophic niche score, potentially due to the low sampling number for *T. maxima* ($n = 9$). Excluding *T. maxima*, the linear regression model indicated that 84.9% ($R^2 = 0.8487$, $P = 0.0262$) of the variance of the average growth rate can be explained by the trophic niche score.

To assess nutritional exchange between symbiotic partners, we examined the difference between giant clam host and symbiont $\delta^{13}\text{C}$ and $\delta^{15}\text{N}$ independently ($\delta^{13}\text{C}_{\text{Host}} - \delta^{13}\text{C}_{\text{Symbiont}}$; $\delta^{15}\text{N}_{\text{Host}} - \delta^{15}\text{N}_{\text{Symbiont}}$)^{5,26}. $\delta^{13}\text{C}_{\text{Host}} - \delta^{13}\text{C}_{\text{Symbiont}}$ values were not normally distributed (Shapiro-Wilk test, $W = 0.97147$, $P = 0.005431$) and heteroscedastic (Levene's test, test statistic = 3.2318, $P = 0.008729$) while $\delta^{15}\text{N}_{\text{Host}} - \delta^{15}\text{N}_{\text{Symbiont}}$ values were normally distributed (Shapiro-Wilk test, $W = 0.98574$, $P = 0.1632$) and homoscedastic (Bartlett's test, $K^2 = 4.8689$, $P = 0.4321$). Both $\delta^{13}\text{C}_{\text{Host}} - \delta^{13}\text{C}_{\text{Symbiont}}$ and $\delta^{15}\text{N}_{\text{Host}} - \delta^{15}\text{N}_{\text{Symbiont}}$ varied significantly across species ($\delta^{13}\text{C}_{\text{Host}} - \delta^{13}\text{C}_{\text{Symbiont}}$; Welch's analysis of variance (ANOVA), test statistic=10.397, $P = 9.709\text{e}^{-7}$; $\delta^{15}\text{N}_{\text{Host}} - \delta^{15}\text{N}_{\text{Symbiont}}$; one-way ANOVA, $F = 16.3$, $P = 1.67\text{e}^{-12}$; Supplementary Fig. 3). *T. gigas* $\delta^{13}\text{C}_{\text{Host}} - \delta^{13}\text{C}_{\text{Symbiont}}$ values were significantly lower than *H. hippopus*, *H. porcellanus*, and *T. squamosa* (Games-Howell post hoc test, $P = 0.0000456$, $P = 0.000887$, and $P = 0.00000266$, respectively) and *H. porcellanus* and *T. derasa* were significantly lower than *T. squamosa* ($P = 0.015$ and $P = 0.001$; Supplementary Fig. 3A). *T. gigas* $\delta^{15}\text{N}_{\text{Host}} - \delta^{15}\text{N}_{\text{Symbiont}}$ values were significantly lower than those of all other species (Tukey's HSD, Supplementary Table 4), and *H. porcellanus* and *T. derasa* $\delta^{15}\text{N}_{\text{Host}} - \delta^{15}\text{N}_{\text{Symbiont}}$ values were significantly

lower than *H. hippopus* and *T. squamosa* (Supplementary Table 4, Supplementary Fig. 3B).

Symbiodiniaceae diversity and community structure

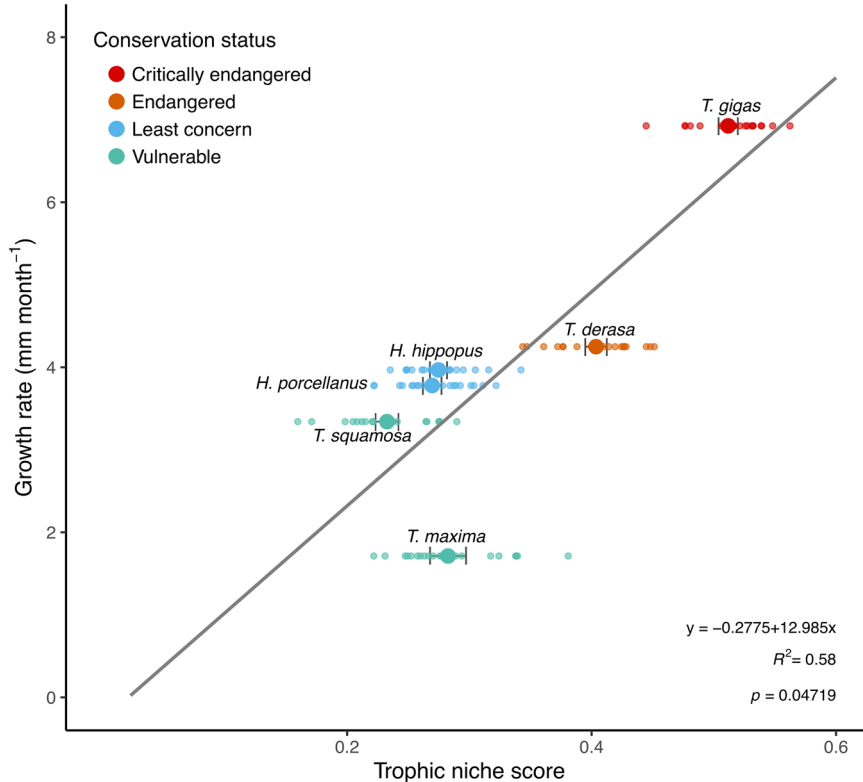
We obtained 3,805,562 sequence reads with an average of 211,420 ($SD \pm 38,407$) reads per library. A total of 16 ITS2 type profiles belonging to three Symbiodiniaceae genera were detected over 18 giant clam samples (Fig. 4). *Cladocopium* was the most common genus and was represented by eight profiles, while genus *Durusdinium* was represented by five profiles, and genus *Symbiodinium* with three profiles. All giant clams hosted a combination of two genera (*Symbiodinium-Cladocopium* or *Cladocopium-Durusdinium*) except for one *H. Hippopus* and one *T. squamosa* individual that contained type profiles representing all three genera (at >1% of the population). One genus typically dominated the community of each giant clam individual.

ITS2 type profiles showed variable distribution among giant clam species. On average, type profile C93a-C93e-C55a was most dominant in *H. porcellanus* (99%), *H. hippopus* (64%), and *T. squamosa* (59%). This type profile co-occurred with A3 (*Symbiodinium tridacnidorum*, a symbiont showing evidence of coevolution with giant clams²⁸; 31%) in *H. hippopus* and D4/D5-D9b-D1bq-D5n (33%) in *T. squamosa*. Symbiodiniaceae in *T. gigas* predominantly consisted of closely related type profiles from genus *Cladocopium* (C93/66-C93e, 33%; C93a-C93e-C93n, 33%; C93a-C93e-C55a, 31%). In *T. derasa*, the dominant type profiles were C93a (66%) and C93a-C93f (26%). *T. maxima* was dominated by profiles C1/C1c-C1a-C1b-C42.2 (81%) and D4/D5-D9b-D1bq-D5n (19%). Non-metric multi-dimensional scaling ordination based on ITS2 type profiles revealed close clustering of *H. hippopus*, *H. porcellanus*, *T. gigas*, and *T. squamosa*, whereas the other two species had greater variability (Supplementary Fig. 4).

Phylogenetic signal analysis

We produced a Bayesian phylogenetic tree, based on 16 genetic mitochondrial and ribosomal sequences¹⁶ that corroborated evolutionary relationships between the six studied clam species supported in previous studies (Fig. 5)^{29,30}. Each node of the tree had a posterior probability greater than 0.89. The phylogenetic signal analyses showed significant patterns in four out of eight ecological traits (Supplementary Fig. 5 and Data 1): mean growth rate ($P = 0.020$; $K = 0.88$), trophic niche score ($P = 0.030$; $K = 1.215$), maximum shell length ($P = 0.031$; $K = 1.026$) and depth ($P = 0.030$; $K = 0.984$).

Fig. 3 | Significant correlation between the trophic niches scores and published mean growth rates of six giant clam species. Color indicates the International Union for Conservation of Nature (IUCN) conservation status of each species, which was critically endangered (red), endangered (orange), vulnerable (blue), or least concern (green)⁴⁷. Small shaded circles represent individual data points (raw trophic niche scores), while plain circles indicate the mean trophic niche score for each species. 89% credible intervals are shown with dark gray error bars. Regression analysis was performed on $n = 6$ biologically independent giant clam species. Growth rates were obtained from Tan et al.^{15,72}.



Discussion

Giant clams are a remarkable group of marine invertebrates, including the largest living bivalve on Earth, *Tridacna gigas*. They act as reef engineers playing a pivotal role in coral reef ecosystems across the Indo-Pacific¹³. However, giant clam populations are undergoing rapid decline due to major anthropogenic stressors, including overexploitation, pollution, and habitat loss, and this vulnerability is further increased by climate change owing to their reliance on symbiosis^{31,32}. Despite growing concern for their conservation¹³, giant clams remain poorly studied. As a taxon, they represent a unique case study to understand the role of nutritional symbioses in the evolution and biogeography of marine species. Giant clams are considered mixotrophic holobionts, acquiring nutrients from both symbiont photosynthesis and suspension feeding^{28,33}, therefore competing amongst themselves and with other benthic taxa for food and space on oligotrophic reefs. This concept of competition is encapsulated in the competitive exclusion principle, which posits that species with overlapping niches compete¹, leading to subtle adaptations to avoid competition, fostering speciation and consequently, sympatry³⁴. Moreover, the host microbiome plays an important role in the ecology and evolution of species, and forming associations with diverse symbionts can confer substantial advantages to the host⁶, leading to trophic niche variations. In giant clams, symbionts are known to translocate a substantial proportion of their photosynthetically fixed carbon to the host³⁵; however, the extent of carbon translocation can vary among symbiont species and strains, introducing further complexity to the nutritional dynamics of the holobiont³⁶. We therefore hypothesized that variation in the relative contributions of auto- and heterotrophic dietary sources, potentially fostered by associations with distinct symbiont assemblages, underpins the ecology and evolution of giant clams and helps explain their biology and biogeography across the Indo-Pacific.

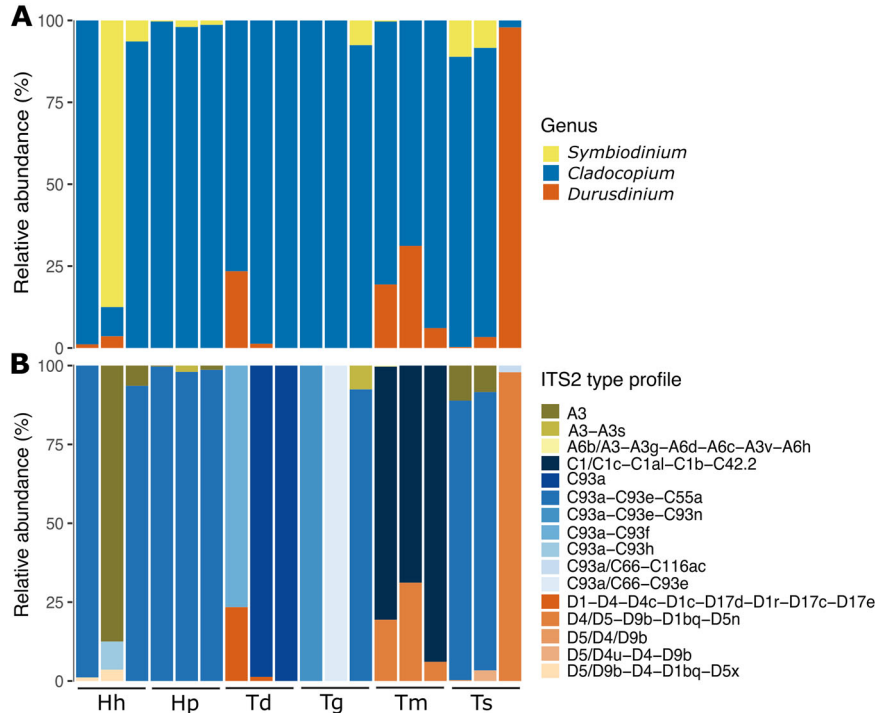
Using a unique common garden, we revealed clear differences in trophic strategy among six co-occurring species of giant clams of comparable age and size within species. Giant clams occupied statistically different regions along a trophic strategy spectrum, demonstrating variation in reliance on symbiont photosynthesis (Fig. 2). *T. squamosa* was positioned near the heterotrophic end of the trophic strategy spectrum, while the other

species displayed a distribution across the mixotrophic range, with *T. derasa* and *T. gigas* falling closer to the autotrophic end of the spectrum. *T. gigas* was the only species exhibiting overlap between host and symbiont standard ellipses area (SEA_B), indicating a closer link between host and symbiont nutrient sources compared to other species (Fig. 1 and Supplementary Table 2). Given that the clams used in this work were all reared and collected from the same site characterized by an open, sandy bottom, the observed variation cannot be explained by micro-environmental differences but rather reflects species-specific differences in trophic strategy. Additionally, all sampled clams were of a similar age (3–4 years old) and of a similar size within species. These results provide overwhelming evidence that giant clam species are not using identical trophic strategies and vary in their reliance on autotrophic and heterotrophic nutrient sources. The dispersion of species along the spectrum supports conceptualizing syntrophic mutualisms as a continuum³⁷ rather than discrete categories (i.e., autotrophy, mixotrophy, or heterotrophy). While mutualisms with photosynthetic algae open additional energetic pathways to marine invertebrates, the evolution of this relationship across multiple taxa has led to intense competition, providing a mechanism for the niche partitioning observed in giant clam species.

Across clam species, host nitrogen isotope values were offset from those of POM by the amount expected for a consumer (~2.5‰)^{38,39}, suggesting that all species obtain some nutrition from filter feeding. Trophic differences across holobionts were instead driven by variation in the $\delta^{15}\text{N}$ values of associated Symbiodiniaceae. In the most autotrophic species (*T. gigas*), the host and symbiont had near identical mean nitrogen values ($\delta^{15}\text{N}_{\text{Host}} - \delta^{15}\text{N}_{\text{Symbiont}} = 0.1 \pm 0.3\text{‰}$), whereas in the more heterotrophic species *T. squamosa*, symbionts had lower $\delta^{15}\text{N}$, resulting in a larger difference from their hosts ($\delta^{15}\text{N}_{\text{Host}} - \delta^{15}\text{N}_{\text{Symbiont}} = 0.7 \pm 0.3\text{‰}$). This suggests differences in the overlap of host and symbiont isotopic niches across clam species were driven by increased nutrient recycling in more autotrophic holobiont species, rather than a decrease in heterotrophy. Given the considerable active filtration capacity of clams^{13,19}, it is unsurprising that POM is an important source of nutrition to the taxon.

Nutrient recycling within mixotrophic holobionts may eliminate isotope fractionation effects that could occur during nutrient translocation or

Fig. 4 | Diversity of Symbiodiniaceae associated with six giant clam species: *Hippopus hippopus* (Hh), *Hippopus porcellanus* (Hp), *Tridacna derasa* (Td), *Tridacna gigas* (Tg), *Tridacna maxima* (Tm), and *Tridacna squamosa* (Ts). Relative abundance of Symbiodiniaceae genera (A) and predicted ITS2 type profiles (B) are shown.



excretion⁴⁰. The similar $\delta^{15}\text{N}$ and $\delta^{13}\text{C}$ values of *T. gigas* hosts and symbionts suggest that either fractionation during translocation is minimal, or that nutrient recycling was extensive enough to negate any fractionation effects. Similarly, lower symbiont $\delta^{15}\text{N}$ values relative to the host could result from the assimilation of isotopically light nitrogenous waste products the host preferentially excretes^{38,39}. Yet, if compounds produced with host waste are in turn shared with the host, these discrete isotope pools will be continually mixed, eliminating fractionation. While an understanding of the fractionation effects of the processes involved in syntrophic mutualisms (e.g. assimilation, synthesis, translocation) would improve the interpretation of our results, it is clear that host and symbiont partners with closer isotope values exhibit more nutrient sharing/recycling than species with divergent values, regardless of the mechanism.

By optimizing their autotrophic capacity, photosymbiotic taxa can achieve high rates of growth^{41,42}. Foundational work by Fitt et al.⁴³ demonstrated that increased autotrophy in *T. derasa*, driven by the addition of dissolved inorganic nitrogen, resulted in enhanced growth. We observed this pattern in the species studied here, where the trophic niche scores correlated significantly with growth rates (Fig. 3). *T. gigas*, the most autotrophic clam that stood out with a trophic niche score >0.5 , outgrows any other clam species⁴⁴, reaching up to 200 kg⁴⁵ (Figs. 2 and 3). Our results confirm that *T. gigas* growth and size are supported through higher nutrient sharing with associated Symbiodiniaceae. Indeed, growth rates of *T. gigas* can double at shallow compared to deep sites⁴⁶ and larger individuals cannot meet their energetic demands through heterotrophic feeding alone²², as the importance of filter feeding declines with increasing clam size³⁵. However, our observations suggest a tradeoff between autotrophy and survival in a changing world. *T. gigas* and *T. derasa* are the only species in this study listed as critically endangered and endangered, respectively, on the IUCN Red List of Threatened species⁴⁷ (Fig. 3), which is mostly due to heavy fishing pressures. They are also the two most autotrophic clams, which may therefore increase their vulnerability under global change scenarios. Similar patterns have been observed with other photosymbiotic taxa, where highly autotrophic corals have been shown to be more susceptible to warming events¹¹. Indeed, during warming events, highly autotrophic corals, such as *Acropora* spp., were the first to show signs of bleaching and exhibited the highest mortality and coral cover loss^{48,49}. Increased sea surface temperatures

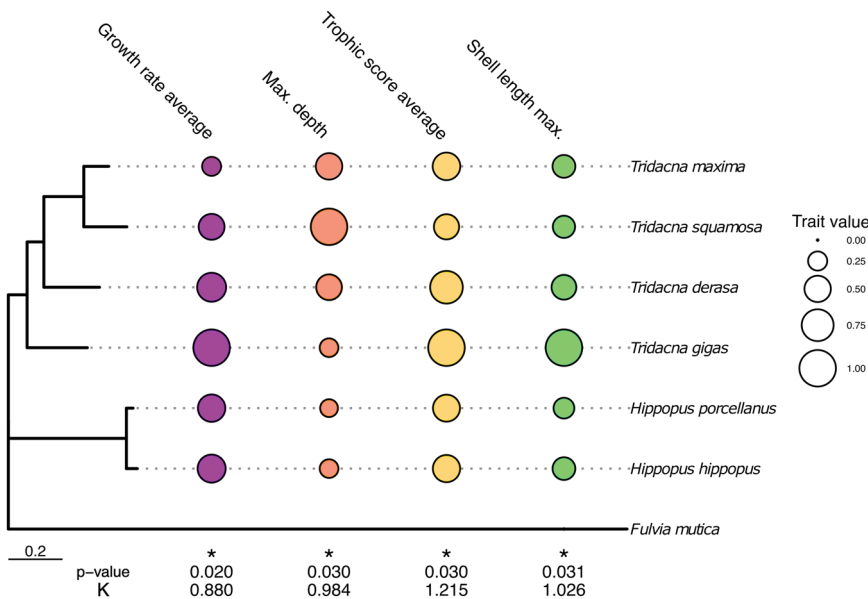
strengthen stratification and thus, limit the availability of essential nutrients and primary production in shallow water coral reef ecosystems⁵⁰, therefore potentially limiting shifts from auto- to heterotrophy⁵¹. This indicates that while autotrophy likely supports high growth rates that confer fitness in space-limiting environments, highly autotrophic species may be less resilient to environmental perturbations, such as warming.

Symbiosis, a key trait that plays a role in host ecology and evolution⁵², is shaped by both environmental conditions⁵³ and host-intrinsic processes, which influence the composition of associated microbiomes¹⁹. Our results suggest clam host control over associated Symbiodiniaceae; species reared in a common environment and inhabiting the same lagoon harbored different genera and ITS2-type profiles (Fig. 4 and Supplementary Fig. 4). Symbiont composition can also vary across the geographic range of the host. *T. maxima*, for example, associated with Symbiodinium in the Red Sea²⁰, Cladocopium and Durusdinium in the Philippines (this study; Fig. 4), and all three genera in French Polynesia¹⁸. Regulation of associated symbiont assemblages may enable giant clams to meet their nutritional needs according to their environment without modification of the host physiology or morphology, providing a mechanism of niche flexibility. In addition, Symbiodiniaceae genera were found to play a role in giant clam growth rates, demonstrating their importance for clams' nutritional needs⁵⁴.

Although no studies have been conducted with clams, previous work with corals and anemones has demonstrated that the role of symbionts in host trophic dynamics varies according to Symbiodiniaceae genera⁵⁵. While the proportion of ITS2 profiles varied among the six species of giant clams (Fig. 4), the three species with similar trophic niche score, *T. squamosa*, *H. hippopus* and *H. porcellanus* also hosted the same dominant ITS2-type profile. This indicates that the Symbiodiniaceae might play a role in giant clam trophic niches, pointing toward the necessity for future studies to explore not just the genera but also the ITS2-type profiles and their functional ecology, as different phylotypes may differ in their capacity to translocate carbon to the host³⁶.

We posit that variation in giant clam nutritional strategy was underpinned by their evolutionary history. We detected a significant phylogenetic signal in mean trophic niche scores ($P < 0.05$, Fig. 5), supporting the hypothesis that trophic niche partitioning played a role in the divergence of species within Tridacninae⁵⁶. Previous work has found that the evolution of

Fig. 5 | Significant ($P < 0.05$) results of a phylogenetic signal analysis for six giant clam species. Traits with a significant phylogenetic signal include the mean trophic niche score (yellow), the mean growth rate (purple), the maximum shell length (green) and the maximum depth (orange). The three traits aside from mean trophic niche score were obtained from Tan et al. 2022. The size of each circle is proportional to the value used for each species in the analysis; the maximum value of each trait was fit to one and the minimum value to 0. The scale bar refers to the number of substitutions per site. *Fulvia mutica*, similar to giant clams, belongs to the Cardiidae family and is included as an outgroup species.



photosymbiosis in giant clams coincided with the expansion of the modern Indo-Pacific coral reef, implying that habitat was a key factor in the development of clam nutritional symbiosis³⁰. Competition for nutrients in oligotrophic tropical seas applied selection pressure for the coupling of heterotrophic and autotrophic metabolisms, maximizing the potential avenues for meeting energetic requirements, while simultaneously reducing competition for scarce food³⁷. Previous studies found that up to six tridacnid can coexist on the same reef, however, they occurred at different depths and substrate types, suggesting adaptation to microhabitats with varying light and/or particulate food availability³⁸. While multiple factors certainly contribute to the distribution of species, partitioning of resources, including autotrophic and heterotrophic nutrient acquisition, largely contribute to the coexistence of marine invertebrates³⁹. In addition, the phylogenetic analysis showed evidence of ecological divergence among the six species of giant clams based on growth rate and maximum shell length (a proxy for maximum size)²² (Fig. 5). More autotrophic clams, particularly *T. gigas*, exhibit faster growth and achieve larger body sizes. Growth rate and body size are important adaptations that play a role in evolution, for instance by increasing competitive abilities^{60,61}. Significant phylogenetic signal in the maximum depth was also revealed, with *T. squamosa* being able to colonize deeper environments (42 m depth) likely due to its predominantly heterotrophic strategy⁶². This is further supported by the species' high resilience to light limitation. Indeed, *T. squamosa* can survive 30 days in total darkness⁶³, which explains its capacity to colonize mesophotic reefs and corroborates our findings regarding its trophic strategy. All these findings align with the ecological theory that anticipates an increased selection for traits that lessen competition through niche differentiation.

This work is a step towards understanding the trophodynamics of symbiotic marine invertebrates, anchored in an evolutionary framework, and providing insights into their vulnerability in the Anthropocene. For the first time to our knowledge, we demonstrated that trophic niche partitioning occurs within giant clam taxa, providing an explanation for the co-occurrence of these foundational species on reefs. Our results also highlighted one potential tradeoff between reliance on autotrophy vs heterotrophy; more autotrophic giant clam species grow faster yet are prone to pressures. Among the six species studied, the more autotrophic and fast-growing species, *T. gigas* and *T. derasa*, are listed as critically endangered and endangered, respectively⁴⁷. This observed decline in the past decades is primarily attributable to overfishing and potentially accelerated by other anthropogenic stressors¹⁷. In addition, recent evidence in other marine invertebrate taxa has demonstrated a link between trophic niche and vulnerability, with more autotrophic corals being more susceptible to thermal

bleaching¹¹. Eutrophication, another major threat of this century, might aggravate the vulnerability of giant clams to climate change by increasing reliance on autotrophy. Therefore, while a commitment to symbiosis can enhance a holobionts nutrient acquisition and growth - a clear advantage in nutrient and space-limited reef ecosystems - will also be an "Achilles' heel" in an increasingly warm and eutrophic world, which could exacerbate the existing vulnerability of giant clams. Trophic strategy may therefore be harnessed as an indicator of species of concern in conservation efforts⁶⁴. Giant clams are also highly impacted by human activities, including overfishing and coastal development³¹. Conservation of these ecosystem engineers, particularly species like *T. gigas*, or *T. derasa* that are highly autotrophic and geographically constrained (Supplementary Fig. 6), requires maintaining environmental factors that enhance autotrophic performance - mitigating seawater temperatures and reducing nutrients and sedimentation, specifically - in addition to curtailing over-harvesting.

Methods

Sample collection

Six giant clam species (*Tridacna gigas*, *Tridacna derasa*, *Hippopus porcellanus*, *Hippopus hippopus*, *Tridacna maxima* and *Tridacna squamosa*) were sampled from a sandy common garden at 2-5 m depth, at the Tabunan lagoon ocean nursery in Semirara Island, Philippines (12° 05'13.62" N, 121° 20'45.66" E, Supplementary Fig. 1). The giant clams were cultured and reared at the Semirara Marine Hatchery Laboratory following standard protocols described in the Giant Clam Hatchery, Ocean Nursery and Stock Enhancement Manual⁶⁵ before being transferred to the ocean nursery at about 3 months old. The sampled giant clams from the Tabunan lagoon were of similar age, between 3 and 4 years old, and were derived from the same spawning cohort for each species. Five of the six giant clam species (*Tridacna gigas*, *Tridacna derasa*, *Hippopus porcellanus*, *Hippopus hippopus* and *Tridacna squamosa*) were sampled in the north of the lagoon, while the *Tridacna maxima* samples were collected less than 400 m away in the southwest of the lagoon. The samples from the five species in the north were collected from a 30 m² area and the *Tridacna maxima* from a 10 m² area. To ensure that both areas had similar conditions, light and temperature hobo loggers were deployed in November 2019 (Supplementary Fig. 2). The mean shell length for each species was as follows: *T. gigas* 31.1 cm (SD ± 3.6), *T. derasa* 19.9 cm (SD ± 3.3), *H. porcellanus* 23.7 cm (SD ± 1.5), *H. hippopus* 24.9 cm (SD ± 4.5), *T. maxima* 16.9 cm (SD ± 1.7), and *T. squamosa* 19.3 cm (SD ± 2.6) (Supplementary Data 2).

To explore niche partitioning across clams, we used a non-lethal sampling protocol in which one small (~approximately 1 × 1 cm) mantle

clip per clam was clamped ~0.5 cm from the edge using sterile hemostat forceps and sterile surgical scissors. Mantles were collected from 27 *T. gigas*, 28 *T. derasa*, 23 *H. porcellanus*, 25 *H. hippopus*, nine *T. maxima* and 26 *T. squamosa* and stored at -40 °C (Supplementary Data 2). Mean wet mass of clips varied from 0.095 ± 0.035 g (*T. derasa*; \pm SD) to 0.177 ± 0.046 g (*H. porcellanus*). On each sampling day, duplicate samples of 3 L of seawater from the Tabunun lagoon were collected and filtered through two 47 mm glass fiber filters (GFF pore size 0.45 μ m) to collect POM (Supplementary Data 1). All the filters were placed in a petri dish and dried at ambient temperature before analysis. All the samples for SIA analysis were collected across three days in November 2019. Additional mantle clips were collected from three individuals of each giant clam species to characterize associated symbiont assemblages (Supplementary Data 2). While initially all samples for symbiont community analysis were from Semirara Island, *T. derasa* and *T. squamosa* samples did not pass library QC, leading to data analysis from hatchery-bred individuals reared at the Silaqui ocean nursery of the University of the Philippines Bolinao Marine Laboratory (Bolinao, Pangasinan, Philippines; Supplementary Data 3). Samples were stored in salt-saturated DMSO-EDTA buffer at 4 °C until DNA extraction.

Laboratory analyses

Mantle samples for SIA were lacerated with a razor blade, placed in 5 ml of Milli-Q water and sonicated (S-150D, BRANSON, United States) for 30 s at 5 W to extract algal symbionts. The supernatant, containing the symbionts, was retained. This process was repeated to maximize symbiont yield. The combined symbiont fractions were centrifuged at 3000 RCF for 10 min. The lacerated mantle was homogenized in 5 ml of Milli-Q water with a Tissue-Tearor (Ultra Turrax T25, IKA labortechnik staufen, Germany) and centrifuged at 2000 RCF for 10 min to separate giant clam host tissue from any residual symbionts. The supernatant was collected and centrifuged again for 5 min at 2200 RCF. The supernatant containing the clean host fraction was kept for analysis. Host and symbiont fractions were stored at -40 °C overnight and then freeze-dried (Alpha 1-4 LCS-Plus, Christ, Germany). Dry clam host tissue (0.9 ± 0.1 mg) and symbionts (0.7 ± 0.1 mg) were weighed into tin capsules. POM from the Tabunun lagoon was scraped off each filter and acidified in silver capsules using two applications of 5 μ L of HPLC-grade 6 N HCL to remove inorganic carbonates. Isotopic ratios of carbon ($\delta^{13}\text{C}$) and nitrogen ($\delta^{15}\text{N}$) were measured at the Stable Isotope Ratio Mass Spectrometry Laboratory at the University of Hong Kong with an environmental analyser (Eurovector EA3028, Italy) coupled to a stable isotope ratio mass spectrometer (Nu Instruments Perspective, UK). Vienna PeeDee belemnite ($\delta^{13}\text{C} = 0.011\text{‰}$) and atmospheric nitrogen ($\delta^{15}\text{N} = 0.004\text{‰}$) were used as standards for C and N, respectively, and accuracy for both was better than 0.1‰.

Total genomic DNA from giant clams was isolated using a Qiagen DNeasy Plant Mini Kit (Qiagen, Germany) following the protocol provided by the manufacturer, with minor adjustments. Briefly, ~1 cm² of mantle tissue was homogenized with a pestle before completing extractions. DNA samples were quantified with a Nanodrop™ spectrophotometer (Thermo-fisher, USA) and sent to Macrogen, South Korea, for library preparation and sequencing. Amplicon libraries were prepared using the Herculase II Fusion DNA Polymerase Nextera XT Index Kit V2 using the primers ITSintfor² and ITS2-reverse³ targeting the ITS2 region of the ribosomal RNA operon. Libraries were sequenced on the Illumina MiSeq platform to generate 2 \times 300 bp reads.

Statistics and reproducibility

SIA statistical analysis. Host and symbiont isotopic niches of the six giant clam species were estimated using Stable Isotope Bayesian Ellipses in R (SIBER) analysis⁶. SIBER analysis was performed on 27 *Tridacna gigas*, 28 *Tridacna derasa*, 23 *Hippopus porcellanus*, 25 *Hippopus hippopus*, 9 *Tridacna maxima*, and 26 *Tridacna squamosa* individuals. SIBER analysis was used to fit ellipse areas (EA) to host and symbiont $\delta^{13}\text{C}$ and $\delta^{15}\text{N}$ values shown on an isotopic biplot. EAs are used to represent isotopic niche, defined as the representative area that a group or species

occupies in isotopic space (typically on a $\delta^{13}\text{C}$ - $\delta^{15}\text{N}$ biplot) and used as a proxy for trophic niche^{67,68}, providing stable results when the number of samples is ≥ 20 ²⁶. We used a Bayesian analysis to generate a posterior distribution of EA. Markov chain Monte Carlo (MCMC) methods were used to generate two chains of 20,000 iterations of probable EAs, starting from a vague Inverse Wishart prior and thinned every 10 iterations. The mode of the last 100 posterior draws of EAs was used as the Bayesian estimate of ellipse area (EA_B)⁶⁹. Standard ellipses area (SEA) encompassing 40% of the data was estimated. In addition, larger ellipses that encompass 95% of the variation of the data (major ellipse area, MEA) were calculated to increase the detection of minimal nutrient sharing. Isotopic biplots are presented with SEAs and MEAs derived from raw data for visual representation.

Based on the SIBER outputs, we used a trophic niche index named Host Evaluation: Reliance on Symbionts (HERS) index, to estimate the relative nutritional importance of the symbionts to host nutrition^{24,25,70}. To do so, this trophic niche index combines the proportional overlap of host (EA_BH) and symbiont (EA_BS) 40% (standard ellipse area; SEA_B) and 95% (major ellipse area; MEA_B) Bayesian ellipses (Eq. 1). According to this index, scores approaching 0 indicate limited nutrient sharing or recycling between host and symbionts, suggesting the host is more heterotrophic. In contrast, scores close to 1 suggest high exchange between the two partners, indicating the host is more autotrophic.

$$\text{Trophic niche index HERS} = \frac{\text{MEA}_B H^{\exp(-\text{MEA}_B S)} + \text{SEA}_B H^{\exp(-\text{SEA}_B S)}}{2} \quad (1)$$

Using stable isotope data we collected from the six clam species, we ran 20 independent SIBER analyses to generate 20 trophic niche scores (HERS) for each species (Supplementary Data 1). Boundaries of the 89% credible intervals (CI) were used to assess statistically significant differences between species⁷¹.

To assess the sharing of carbon and nitrogen independently, we subtracted the isotope value of the symbiont from that of its paired host ($\delta^{13}\text{C}_{\text{Host}} - \delta^{13}\text{C}_{\text{Symbiont}}$, $\delta^{15}\text{N}_{\text{Host}} - \delta^{15}\text{N}_{\text{Symbiont}}$)^{5,26}. The distributions of $\delta^{13}\text{C}_{\text{Host}} - \delta^{13}\text{C}_{\text{Symbiont}}$ and $\delta^{15}\text{N}_{\text{Host}} - \delta^{15}\text{N}_{\text{Symbiont}}$ were assessed visually with Q-Q plots and statistically with Shapiro-Wilk tests, while scedasticity was evaluated with either a Bartlett's test if data were normal or a Levene's test if data were not normally distributed. Statistical differences between the $\delta^{13}\text{C}_{\text{Host}} - \delta^{13}\text{C}_{\text{Symbiont}}$ and $\delta^{15}\text{N}_{\text{Host}} - \delta^{15}\text{N}_{\text{Symbiont}}$ of different species were determined using one-way ANOVAs for normally distributed and homoscedastic data, or a Welch's ANOVAs for non-normal and heteroscedastic data. If significant differences between species were detected, pairwise comparisons were evaluated using either Tukey's HSD tests or Games-Howell Post-hoc tests, again depending on the distribution and scedasticity of the datasets. The distance between host and symbiont ellipse centroids (DEC) was also calculated with lower values indicative of more autotrophy and higher values indicative of more heterotrophy¹¹. Finally, significant differences in the relative placement of host and symbiont isotopic niches were determined using residual permutation procedures²⁷. We examined whether clam trophic scores were correlated with published growth rates^{15,72} (Supplementary Data 1) using a linear regression (generalized linear model). All isotope analyses were conducted in R version 4.2.1 using RStudio v.1.4.1103⁷³.

ITS2 sequence analysis. Sequence analysis was conducted in the SymPortal framework⁷⁴ to predict ITS2 type profiles as proxies for putative Symbiodiniaceae genotypes. Raw paired reads were subjected to quality control (QC) using mothur v.1.39.5^{75,76}. Reads were screened for Symbiodiniaceae sequences within the range of 184–310 bp and algorithmically searched in a genus-separated manner using the BLAST+ suite of executables⁷⁶ and Minimum Entropy Decomposition (MED)⁷⁷. Post-QC, ITS2 sequences were loaded to both local and remote SymPortal databases to identify specific sets of ITS2 sequences re-occurring in

multiple samples called defining intragenomic variants (DIVs). The presence and abundance of these DIVs were used to define the ITS2 type profiles. Raw data are available in the Bioproject PRJNA749183, with BioSample and Sequence Read Archive (SRA) numbers listed in Supplementary Data 3. To visualize Symbiodiniaceae community structures, non-metric multidimensional scaling based on Bray-Curtis dissimilarity measures from abundance data was plotted (Supplementary Fig. 4).

Phylogenetic analysis. A phylogenetic signal analysis to investigate evolutionary patterns of ecological divergence among species^{10,12} was realized by pairing a giant clam phylogeny with 8 ecological traits (Supplementary Data 1). The 18S rRNA gene and 15 mitochondrial genes of the six studied giant clams and a cardiid outgroup species (*Fulvia mutica*) were obtained from Tan et al.¹⁶. Model substitution for each of the 16 gene partitions was selected with the Bayesian information criterion (BIC) using jModelTest v2.1.10^{78,79}. A dated phylogenetic tree was constructed with MrBayes version 3.2.7a⁸⁰ from four independent Markov Chain Monte Carlo (MCMC) analyses, each containing four chains of two million cycles sampled every 100 cycles and trimmed from the first 25%. The phylogenetic tree was drawn from the resulting posterior distribution.

The multiPhylosignal function from the R package *picante*⁸¹, was used to detect significant phylogenetic patterns in eight different ecological traits (Supplementary Data 1), using a bootstrapping technique with 720 (6!) replacements. Each final trait result was extracted from the mean of 1000 independent multiPhylosignal analyses (Supplementary Fig. 5). Of the eight traits, three were obtained from the literature (mean growth rate, maximum shell length and maximum depth)¹⁶, one (occurrence in different provinces) was determined by matching published occurrences of giant clam species¹⁷ to established Marine Ecoregions of the World⁸² resulting in the number of ecoregions each clam inhabits (Supplementary Data 1), and four were determined in this study (Distance to the ellipse centroids DEC, mean $\delta^{15}\text{N}$, mean $\delta^{13}\text{C}$, and trophic niche score). K values greater or equal to 1 demonstrated a close fit to the phylogenetic relationship between species, while values close to 0 indicated a pattern abnormally different from the phylogenetic tree^{83,84}.

Ethics approval

Our study brings together authors from different countries, including scientists based in the country where the study was carried out. We acknowledge that local researchers were involved throughout the research process, and our research could not have been done without them.

Reporting summary

Further information on research design is available in the Nature Portfolio Reporting Summary linked to this article.

Data availability

All sequences generated for this study were deposited under Bioproject PRJNA749183 BioSample and Sequence Read Archive (SRA) accession number are provided in Supplementary Data 3. Data needed to evaluate the conclusions in the paper are present in the paper and/or the Supplementary Materials. Data are also accessible at [https://doi.org/10.5281/zenodo.17637054⁸⁵](https://doi.org/10.5281/zenodo.17637054).

Code availability

Analysis code to support the findings of the paper is available on GitHub (<https://github.com/iguibert/Trophic-niche-partitioning-in-giant-clams.git>) and also at [https://doi.org/10.5281/zenodo.17637054⁸⁵](https://doi.org/10.5281/zenodo.17637054).

Received: 3 February 2025; Accepted: 20 November 2025;

Published online: 06 December 2025

References

1. Gause, G. F. *The Struggle for Existence*. vol. 120 (Hafner, 1934).
2. Haine, E. R. Symbiont-mediated protection. *Proc. R. Soc. B Biol. Sci.* **275**, 353–361 (2008).
3. Fisher, R. M., Henry, L. M., Cornwallis, C. K., Kiers, E. T. & West, S. A. The evolution of host-symbiont dependence. *Nat. Commun.* **8**, 15973 (2017).
4. Douglas, A. E. *The Symbiotic Habit*. (2010).
5. Muscatine, L., Porter, J. W. & Kaplan, I. R. Resource partitioning by reef corals as determined from stable isotope composition—I. $\delta^{13}\text{C}$ of zooxanthellae and animal tissue vs depth. *Mar. Biol.* **100**, 185–193 (1989).
6. Rowan, R. Diversity and ecology of zooxanthellae on coral reefs. *J. Phycol.* **34**, 407–417 (1998).
7. Trench, R. K. Microalgal-Invertebrate symbiosis: a review. *Endocytobiosis Cell Res.* **175**, 135–175 (1993).
8. Hawkins, A. J. S. & Klumpp, D. W. Nutrition of the giant clam *Tridacna gigas* (L.). II. Relative contributions of filter-feeding and the ammonium-nitrogen acquired and recycled by symbiotic alga towards total nitrogen requirements for tissue growth and metabolism. *J. Exp. Mar. Biol. Ecol.* **190**, 263–290 (1995).
9. Rowan, R. Thermal adaptation in reef coral symbionts. *Nature* **430**, 742 (2004).
10. Baker, D. M. et al. Productivity links morphology, symbiont specificity and bleaching in the evolution of Caribbean octocoral symbioses. *ISME J.* **9**, 2620–2629 (2015).
11. Conti-Jerpe, I. E. et al. Trophic strategy and bleaching resistance in reef-building corals. *Sci. Adv.* **6**, eaaz5443 (2020).
12. Freeman, C. J. et al. Microbial symbionts and ecological divergence of Caribbean sponges: a new perspective on an ancient association. *ISME J.* **14**, 1571–1583 (2020).
13. Neo, M. L., Eckman, W., Vicentuan, K., Teo, S. L. M. & Todd, P. A. The ecological significance of giant clams in coral reef ecosystems. *Biol. Conserv.* **181**, 111–123 (2015).
14. Alcazar, S. N. Observation on predators of giant clams (Bivalvia: Family Tridacnidae). *Silliman J.* **33**, 54–57 (1986).
15. Tan, E. Y. W., Neo, M. L. & Huang, D. Assessing taxonomic, functional and phylogenetic diversity of giant clams across the Indo-Pacific for conservation prioritization. *Divers Distrib.* **1**, 15 (2022).
16. Tan, E. Y. W., Quek, Z. B. R., Neo, M. L., Fauvelot, C. & Huang, D. Genome skimming resolves the giant clam (Bivalvia: Cardiidae: Tridacninae) tree of life. *Coral Reefs* **1**, 14 (2021).
17. Neo, M. L. et al. Giant clams (Bivalvia: Cardiidae: Tridacninae): a comprehensive update of species and their distribution, current threats and conservation status. *Oceanogr. Mar. Biol.: Annu. Rev.* **55**, 87–387 (2017).
18. Guibert, I., Lecellier, G., Torda, G., Pochon, X. & Berteaux-Lecellier, V. Metabarcoding reveals distinct microbiotypes in the giant clam *Tridacna maxima*. *Microbiome* **8**, 57 (2020).
19. Ikeda, S. et al. Zooxanthellal genetic varieties in giant clams are partially determined by species-intrinsic and growth-related characteristics. *PLoS One* **12**, e0172285 (2017).
20. Pappas, M. K., He, S., Hardenstine, R. S., Kanee, H. & Berumen, M. L. Genetic diversity of giant clams (*Tridacna* spp.) and their associated *Symbiodinium* in the central Red Sea. *Mar. Biodivers.* **47**, 1209–1222 (2017).
21. Mies, M. et al. Anatomical complexity allows for heat-stressed giant clams to undergo symbiont shuffling at both organism and organ levels. *Mar. Biol.* **172**, 1–14 (2025).
22. Klumpp, D. W., Bayne, B. L. & Hawkins, A. J. S. Nutrition of the giant clam *tridacna gigas* (L.). I. Contribution of filter feeding and photosynthates to respiration and growth. *J. Exp. Mar. Biol. Ecol.* **155**, 105–122 (1992).
23. Klumpp, D. W. & Griffith, C. L. Contributions of phototrophic and heterotrophic nutrition to the metabolic and growth requirements of four species of giant clam (Tridacnidae). *Mar. Ecol. Prog. Ser.* **115**, 103–116 (1994).

24. Guibert, I. et al. Trophic niche partitioning in symbiotic marine invertebrates. <https://doi.org/10.1101/2024.02.05.578332> (2024).

25. Pons, L. et al. Host Evaluation: reliance on symbionts: a new metric for quantifying nutrient exchange in nutritional mutualisms. *Methods Ecol. Evol.* **16**, 2048–2066 (2025).

26. Syväranta, J., Lensu, A., Marjomäki, T. J., Oksanen, S. & Jones, R. I. An empirical evaluation of the utility of convex hull and standard ellipse areas for assessing population niche widths from stable isotope data. *PLoS One* **8**, 1–9 (2013).

27. Turner, T. F., Collyer, M. L. & Krabbenhoft, T. J. A general hypothesis-testing framework for stable isotope ratios in ecological studies. *Ecology* **91**, 2227–2233 (2010).

28. Mies, M. Evolution, diversity, distribution and the endangered future of the giant clam–Symbiodiniaceae association. *Coral Reefs* **38**, 1067–1084 (2019).

29. Benzie, J. A. H. & Williams, S. T. Phylogenetic relationships among giant clam species (Mollusca: Tridacnidae) determined by protein electrophoresis. *Mar. Biol.* **132**, 123–133 (1998).

30. Li, J. et al. Shedding light: A phylotranscriptomic perspective illuminates the origin of photosymbiosis in marine bivalves. *BMC Biol.* **20**, 1–15 (2020).

31. Neo, M. L. *Conservation of Giant Clams (Bivalvia: Cardiidae)*. Encyclopedia of the World's Biomes. <https://doi.org/10.1016/b978-0-12-409548-9.11780-4>. (Elsevier Inc. 2020).

32. Watson, S. A. & Neo, M. L. Conserving threatened species during rapid environmental change: Using biological responses to inform management strategies of giant clams. *Conserv Physiol.* **9**, coab082 (2021).

33. Sturaro, N., Hsieh, Y. E., Chen, Q., Wang, P. L. & Denis, V. Trophic plasticity of mixotrophic corals under contrasting environments. *Funct. Ecol.* **35**, 2841–2855 (2021).

34. Hunt, D. E. et al. Resource Partitioning and sympatric differentiation among closely related bacterioplankton. *Science* **320**, 1081–1086 (2008).

35. Lucas, J. S. The biology, exploitation, and mariculture of giant clams (Tridacnidae). *Rev. Fish. Sci.* **2**, 181–223 (1994).

36. Stat, M., Morris, E. & Gates, R. D. Functional diversity in coral-dinoflagellate symbiosis. *Proc. Natl. Acad. Sci. USA* **105**, 9256–9261 (2008).

37. Palardy, J. E., Rodrigues, L. J. & Grottoli, A. G. The importance of zooplankton to the daily metabolic carbon requirements of healthy and bleached corals at two depths. *J. Exp. Mar. Biol. Ecol.* **367**, 180–188 (2008).

38. DeNiro, M. J. & Epstein, S. Influence of diet on the distribution of nitrogen isotopes in animals. *Geochim Cosmochim. Acta* **45**, 341–351 (1981).

39. Minagawa, M. & Wada, E. Stepwise enrichment of ^{15}N along food chains: Further evidence and the relation between $\delta^{15}\text{N}$ and animal age. *Geochim Cosmochim. Acta* **48**, 1135–1140 (1984).

40. Reynaud, S. et al. Effect of light and feeding on the nitrogen isotopic composition of a zooxanthellate coral: Role of nitrogen recycling. *Mar. Ecol. Prog. Ser.* **392**, 103–110 (2009).

41. Huston, M. A. Patterns of species diversity on coral reefs. *Annu. Rev. Ecol. Syst.* **16**, 149–177 (1985).

42. Muscatine, L. & Porter, J. W. Reef corals: mutualistic symbioses adapted to nutrient-poor environments. *Bioscience* **27**, 454–460 (1977).

43. Fitt, W. K., Heslinga, G. A. & Watson, T. C. Utilization of dissolved inorganic nutrients in growth and mariculture of the tridacnid clam *Tridacna derasa*. *Aquaculture* **109**, 27–38 (1993).

44. Yonge, C. M. Functional morphology and evolution in the Tridacnidae (Mollusca: Bivalvia: Cardiacea). *Rec. Aust. Mus.* **33**, 735–777 (1982).

45. Copland, J. W. & Lucas, J. S. *Giant Clams in Asia and the Pacific. Giant clams in Asia and the Pacific*. ACIAR Monograph 9 (1988).

46. Fitt, W. K. et al. *The Biology and Mariculture of Giant Clams: A Workshop Held in Conjunction with 7th International Coral Reef Symposium 21–26 June 1992, Guam, USA. ACIAR proceedings* (1993).

47. IUCN. The IUCN Red List of Threatened Species. 2024-2 <https://www.iucnredlist.org/> (2024).

48. Loya et al. Coral bleaching: the winners and the losers. *Ecol. Lett.* **4**, 122–131 (2001).

49. Hughes, T. P. et al. Global warming transforms coral reef assemblages. *Nature* **556**, 492–496 (2018).

50. Moore, C. M. et al. Processes and patterns of oceanic nutrient limitation. *Nat. Geosci.* **6**, 701–710 (2013).

51. Ezzat, L. et al. Nutrient starvation impairs the trophic plasticity of reef-building corals under ocean warming. *Funct. Ecol.* **33**, 643–653 (2019).

52. Van Oppen, M. J. H. & Medina, M. Coral evolutionary responses to microbial symbioses: Coral-microbe symbiosis. *Philos. Trans. R. Soc. B Biol. Sci.* **375**, 1–8 (2020).

53. DeBoer, T., Baker, A., Erdmann, M., Jones, P. & Barber, P. Patterns of *Symbiodinium* distribution in three giant clam species across the biodiverse Bird's Head region of Indonesia. *Mar. Ecol. Prog. Ser.* **444**, 117–132 (2012).

54. Long, C. et al. Effects of Symbiodiniaceae Phylotypes in Clades A–E on Progeny Performance of Two Giant Clams (*Tridacna squamosa* and *T. crocea*) During Early History Life Stages in the South China Sea. *Front. Mar. Sci.* **8**, 633761 (2021).

55. Sproles, A. E. et al. Sub-cellular imaging shows reduced photosynthetic carbon and increased nitrogen assimilation by the non-native endosymbiont *Durusdinum trenchii* in the model cnidarian *Aiptasia*. *Environ. Microbiol.* **22**, 3741–3753 (2020).

56. Rocap, G. et al. Genome divergence in two *Prochlorococcus* ecotypes reflects oceanic niche differentiation. *Nature* **424**, 1042–1047 (2003).

57. Muratore, D. et al. Complex marine microbial communities partition metabolism of scarce resources over the diel cycle. *Nat. Ecol. Evol.* **1**, 20 (2022).

58. Hardy, J. & Hardy, S. Ecology of *Tridacna* in Palau. *Pac. Sci.* **23**, 467–472 (1969).

59. Foffa, D., Young, M. T., Stubbs, T. L., Dexter, K. G. & Brusatte, S. L. The long-term ecology and evolution of marine reptiles in a Jurassic seaway. *Nat. Ecol. Evol.* **2**, 1548–1555 (2018).

60. Olinger, L. K., Chaves-Fonnegra, A., Enochs, I. C. & Brandt, M. E. Three competitors in three dimensions: photogrammetry reveals rapid overgrowth of coral during multispecies competition with sponges and algae. *Mar. Ecol. Prog. Ser.* **657**, 109–121 (2021).

61. Shingleton, A. W. Evolution and the regulation of growth and body size. In *Mechanisms of Life History Evolution* 43–55 <https://doi.org/10.1093/acprof:oso/9780199568765.003.0004> (2013).

62. Jantzen, C. et al. Photosynthetic performance of giant clams, *Tridacna maxima* and *T. squamosa*, Red Sea. *Mar. Biol.* **155**, 211–221 (2008).

63. Ip, Y. K., Boo, M. V., Mies, M. & Chew, S. F. The giant clam *<math>i>Tridacna squamosa* quickly regenerates iridocytes and restores symbiont quantity and phototrophic potential to above-control levels in the outer mantle after darkness-induced bleaching. *Coral Reefs* **41**, 35–51 (2022).

64. Skinner, C., Cobain, M. R. D., Zhu, Y., Wyatt, A. S. J. & Polunin, N. V. C. Progress and direction in the use of stable isotopes to understand complex coral reef ecosystems: a review. *Oceanogr. Mar. Biol.* **1**, 94 (2022).

65. Mingo-Licuanan, S. S. & Gomez, E. D. *Giant Clam Hatchery, Ocean Nursery and Stock Enhancement. Aquaculture Extension Manual No. 37* (2007).

66. Jackson, A. L., Inger, R., Parnell, A. C. & Bearhop, S. Comparing isotopic niche widths among and within communities: SIBER—Stable Isotope Bayesian Ellipses in *R*. *J. Anim. Ecol.* **80**, 595–602 (2011).

67. Bearhop, S., Adams, C. E., Waldron, S., Fuller, R. A. & Macleod, H. Determining trophic niche width: a novel approach using stable isotope analysis. *J. Anim. Ecol.* **73**, 1007–1012 (2004).

68. Newsome, S. D., Martinez del Rio, C., Bearhop, S. & Phillips, D. L. A niche for isotopic ecology. *Front Ecol. Environ.* **5**, 429–436 (2007).

69. Swanson, H. K. et al. A new probabilistic method for quantifying n-dimensional ecological niches and niche overlap. *Ecology* **96**, 318–324 (2015).

70. Chei, E., Conti-Jerpe, I. E., Pons, L. & Baker, D. Changes within the coral symbiosis underpin seasonal trophic plasticity in reef corals. *ISME Commun.* <https://doi.org/10.1093/ismeco/ycae162> (2025).

71. Makowski, D., Ben-Shachar, M. & Lüdecke, D. bayestestR: Describing effects and their uncertainty, existence and significance within the Bayesian framework. *J. Open Source Softw.* **4**, 1541 (2019).

72. Tan, E. Y. W., Neo, M. L. & Huang, D. Assessing taxonomic, functional, and phylogenetic diversity of giant clams across the Indo-Pacific for conservation prioritisation [Data set]. *Diversity and Distributions* vol. 28 2124–2138 (2022).

73. Team, R. C. R.: A language and environment for statistical computing. <https://www.r-project.org/> (2020).

74. Hume, B. C. C. et al. SymPortal: a novel analytical framework and platform for coral algal symbiont next-generation sequencing ITS2 profiling. *Mol. Ecol. Resour.* **19**, 1063–1080 (2019).

75. Schloss, P. D. et al. Introducing mothur: open-source, platform-independent, community-supported software for describing and comparing microbial communities. *Appl. Environ. Microbiol.* **75**, 7537–7541 (2009).

76. Camacho, C. et al. BLAST+: architecture and applications. *BMC Bioinforma.* **10**, 421 (2009).

77. Eren, A. M. et al. Minimum entropy decomposition: Unsupervised oligotyping for sensitive partitioning of high-throughput marker gene sequences. *ISME J.* **9**, 968–979 (2015).

78. Darriba, D., Taboada, G. L., Doallo, R. & Posada, D. JModelTest 2: more models, new heuristics and parallel computing. *Nat. Methods* **9**, 772 (2012).

79. Nascimento, F. F., Reis, M., Dos & Yang, Z. A biologist's guide to Bayesian phylogenetic analysis. *Nat. Ecol. Evol.* **1**, 1446–1454 (2017).

80. Ronquist, F. et al. MrBayes 3.2: Efficient Bayesian phylogenetic inference and model choice across a large model space. *Syst. Biol.* **61**, 539–542 (2012).

81. Kembel, S. W. et al. Picante: R tools for integrating phylogenies and ecology. *Bioinformatics* **26**, 1463–1464 (2010).

82. Spalding, M. D. et al. Marine ecoregions of the world: a bioregionalization of coastal and shelf areas. *Bioscience* **57**, 573–583 (2007).

83. Revell, L. J., Harmon, L. J. & Collar, D. C. Phylogenetic signal, evolutionary process, and rate. *Syst. Biol.* **57**, 591–601 (2008).

84. Blomberg, S. P., Garland, T. & Ives, A. R. Testing for phylogenetic signal in comparative data: Behavioral traits are more labile. *Evolution* **57**, 717–745 (2003).

85. Guibert, I. et al. iguibert/Trophic-niche-partitioning-in-giant-clams: Trophic niche partitioning in giant clams (V11_2025). Zenodo <https://doi.org/10.5281/zenodo.1763704> (2025).

Acknowledgements

We deeply thank Dr. R. Estrellada, Director of the Semirara Marine Hatchery Laboratory (SMHL), as well as the staff of SMHL for hosting Dr. I. Guibert and for field assistance; J. I. P. Baquiran for logistics in the field; O. So for helping

with all necessary orders; A. Y. T. Chan for technical assistance at the University of Hong Kong; Dr. O. Habimana for lending materials; and Dr. S. McIlroy for valuable discussion. This study was funded by the University of Hong Kong Division of Ecology and Biodiversity PDF Research Award, by the General Research Fund (GRF-17108620), by the Environment and Conservation Fund and the Collaborative Research Fund (ECF-67/2016 and CRF7G_C7013-19G) and by the Department of Science and Technology Philippine Council for Agriculture, Aquatic and Natural Resources Research and Development (DOST-PCAARRD; QMSR-MRRD-MEC-295-1449, 314-1542 and 314-1545).

Author contributions

I.G. designed the study. I.G. and D.M.B. secured funding for the study. I.G., S.L.S., P.C. and C.C. carried out field sampling and helped with logistics. L.P., I.G., I.C.J. and K.T. performed the laboratory work. L.P., I.C.J., K.T. and I.G. performed the analysis. I.G. wrote the first draft of the manuscript, and all authors contributed to the final manuscript.

Competing interests

The authors declare no competing interests.

Additional information

Supplementary information The online version contains supplementary material available at <https://doi.org/10.1038/s42003-025-09313-z>.

Correspondence and requests for materials should be addressed to David Michael Baker.

Peer review information *Communications Biology* thanks Lee Li Keat and the other anonymous reviewer(s) for their contribution to the peer review of this work. Primary Handling Editors: Eoin O'Gorman and Michele Repetto. A peer review file is available.

Reprints and permissions information is available at <http://www.nature.com/reprints>

Publisher's note Springer Nature remains neutral with regard to jurisdictional claims in published maps and institutional affiliations.

Open Access This article is licensed under a Creative Commons Attribution-NonCommercial-NoDerivatives 4.0 International License, which permits any non-commercial use, sharing, distribution and reproduction in any medium or format, as long as you give appropriate credit to the original author(s) and the source, provide a link to the Creative Commons licence, and indicate if you modified the licensed material. You do not have permission under this licence to share adapted material derived from this article or parts of it. The images or other third party material in this article are included in the article's Creative Commons licence, unless indicated otherwise in a credit line to the material. If material is not included in the article's Creative Commons licence and your intended use is not permitted by statutory regulation or exceeds the permitted use, you will need to obtain permission directly from the copyright holder. To view a copy of this licence, visit <http://creativecommons.org/licenses/by-nc-nd/4.0/>.

© The Author(s) 2025